EuroRV3: EuroVis Workshop on Reproducibility, Verification, and Validation in Visualization (2016)
K. Lawonn, M. Hlawitschka, and P. Rosenthal (Editors)

OphthalVis - Making Data Analytics of Optical Coherence Tomography Reproducible

Paul Rosenthal[1], Marc Ritter[2], Danny Kowerko[2], and Christian Heine[3]

[1]Visual Computing Laboratory, Technische Universität Chemnitz, Germany
[2]Juniorprofessur Media Computing, Technische Universität Chemnitz, Germany
[3]AG Computational Topology, TU Kaiserslautern, Germany

Abstract

In this paper, we discuss the issues of the current state of the art in optical coherence tomography with respect to reproducibility. We present our findings about the internal computations and data storage methods of the currently used devices. The gained knowledge was used to implement a tool to read a variety of OCT file formats and reproduce the visualizations used in daily clinical routine.

1. Introduction

The human macula is a highly specialized region in the central part of the retina of the human eye. It is the only part of the retina that provides precise vision and enables humans to read or recognize faces. Hence, medical conditions concerning the macula are the most common cause for permanent visual impairment in industry nations nowadays. On the other hand, there are more and more enhanced examination methods evolving, allowing very detailed and in-depth measurements of anatomic properties. One of these methods is the optical coherence tomography (OCT) [HSL*91]. It is an extension of the fundus photography, where the retina is photographed using a flashlight and a microscopic camera. The light, coming from the retina, is analyzed on the light-wave level using interferometry. Since the retinal tissue is not completely opaque and the different retinal layers exhibit different optical properties, it is possible to extract the layer structure up to a depth of several hundred micrometers. Since such analyses can be performed for each point on the retina and generate a respective depth profile, the resulting data is either a single slice through the retina or a set of slices, i.e. a three-dimensional scalar data set, representing reflectivity of the tissue.

In the clinical context of ophthalmology, two of the most important retinal layers are the retinal pigment epithelium (RPE) and the inner limiting membrane (ILM), which can be quite reliably extracted from OCT data. Many medical conditions, like diabetic retinopathy, retinal vein occlusion, or age-related macular degeneration, can be detected, especially by analyzing the RPE and ILM layers. Furthermore, it is possible to proactively monitor the therapy process of patients with these diseases. This is why OCT is nowadays widely accepted and used in ophthalmological diagnosis.

1.1. OCT Devices

Due to the wide usage, there exists a huge market for OCT scanning devices. However, the market is in large part dominated by only five device manufacturers: Heidelberg Engineering, Zeiss, Topcon, Nidek, and Eyetec. Surprisingly, there is no common data format which could be used by all scanners. Every manufacturer uses it's own OCT data format for storage and transport. Furthermore, there are only a few manufacturers providing documentation for their file formats. Some even try to mystify their data formats by claiming high complexity, effectively discouraging uncontrolled data reading efforts. Consequently, each scanning device is accompanied by a visualization and data-management software, only able to process the device's data respectively. Direct comparisons between scans of different machines are not possible, actually complicating the examination of the progress of patients by different physicians.

And although all used devices and programs are certified, it remains unclear what they exactly measure and how they process their raw data. As far as we have encountered, there is no documentation with regard to this available from any major device manufacturer. Consequently, it remains not only unclear how the output data is stored but it also remains irreproducible how the output data is internally generated. That this is an actual problem in practice, which can be observed when scanning the same eye consecutively with two different devices. In our experiments, we could detect a difference of more than 10% in this procedure between the measurements of a Zeiss and a Topcon device. According to this, it remains unclear how far the stated micrometers in the data represent actual physical properties.

DOI: 10.2312/eurorv3.20161109

2. Data Landscape

We studied the data formats for the devices of the five dominating manufacturers. Also with quite some efforts, we could not obtain specifications for the used formats. Therefore, we had to analyze a given group of data sets together with data exports and screen shots of the manufacturer's programs in order to build our own code for importing such data. Our success varied with each format's difficulty. We found that while earlier products tend to use proprietary formats, more recent products build more on open or well-known formats for images, compression, and meta data. However, a clear standard is lacking, both in what to record and how it is encoded, posing a challenge not only to interoperability, but also to archival.

For each data format, we attempted to extract at least the tomogram, fundus image, contour geometry, as well as the following meta data:

- subject name, sex, and date of birth
- acquisition data and laterality (left or right eye)
- tomogram voxel and fundus pixel dimensions in micrometers, registration of fundus and tomogram data, macula center.

The data format from Nidek was the simplest. It contained most meta data in an XML file, image data in uncompressed BMP files, and contour geometry in a proprietary binary format. All files are contained in a common directory using a fixed naming scheme. Eyetec data is a ZIP-compressed set of files following a naming scheme. It uses XML files for meta data, proprietary binary formats for the raw images and contour data, the latter two being additionally compressed using GZIP. Topcon uses a single file with a proprietary binary format for meta data, image data, and contour data. Image data uses JPEG2000 compression. Heidelberg Engineering's E2E format uses a single file with a proprietary binary format. Its tomogram data uses raw storage of unsigned 16-bit floating point values. In contrast, Zeiss data is build on the DICOM framework. It uses many non-standard DICOM tags and a kind of JPEG compression lacking a JPEG header for image data. This renders the file non-standard and for our purposes unsuitable. We therefore removed Zeiss data from our consideration.

Comparing across formats, OCT data varies a lot, even between different machine generations of the same manufacturer: the area of the eye under observation ranges from 6 mm $\times$ 4.5 mm to 12 mm $\times$ 9 mm, the number of tomogram slices from as little as 5 up to 128, the slice resolution from 512×480 pixels up to 1024×885 pixels, and the number of contours from 3 to 7. Quite often it appears that the manufacturer's programs hard-code which contours describe ILM and RPE surface, and how to register fundus and tomogram images. While some formats store the tomogram data registered for depth and macula center (e.g. Topcon), others store tomogram data before registration (e.g. Heidelberg E2E). This information is necessary to compute macula thickness correctly. Some programs also seem to determine the macula center after loading, since we could not find such information in the meta data (e.g. Nidek and Eyetec). Most formats store contour data as pixel coordinates relative to the tomogram. However, Heidelberg E2E uses floating point numbers denoting the depth in micrometers. Finally, each format seems to use slightly different intensity to gray value profiles, which does not affect visual interpretation of the data, but possibly affects thresholds and parameters for automatic image processing.

2.1. UOCTE

All knowledge gained in the OphthalVis project about the different file formats was used to implement the C++ library UOCTE (Unified OCT Explorer), for importing the different current file formats. The respective code is freely available at `http://www.bitbucket.org/uocte`. In addition, we propose UOCTML as a new simple data format to store the bare essentials of OCT data in a unified way for interoperability. It consists of an XML file plus a set of binary files for uncompressed storage of fundus, tomogram, and contour data. The XML file contains meta data and references the binary data. Our converter stores only a core of meta data – we ignored the plethora of other meta data each format provided – but the format is not limited in this respect. The wiki of the UOCTE repository provides a detailed specification of the UOCTML file format. With the functionality of UOCTE, to our knowledge, the first time it is possible to store OCT data of different manufacturers in a unified data format and implement a unified data analytics and visualization pipeline for OCT data. However, it also gets even more prevalent how problematic the different calibrations and internal computation procedures of the different manufacturers, described in Section 1.1, are for clinical use.

In the following, we present some extensions of the data conversion tool that allow already to emulate the current manufacturer-bound work flows and even extend them.

3. Data Processing

A basic requirement to determine the degree of damage in the context of macula is the identification and analysis of the different retinal layers in the OCT scans. Here, the correct detection of the RPE is crucial to automatically determine this degree of damage. As discussed in Section 2, it is not always the case that the detected retinal layers are stored in the data. Hence, it is necessary to implement a reliable detection of retinal layers to allow for a manufacturer-independent OCT work flow. In Kahl et at. [KRR14], we introduce a two-dimensional image processing algorithm based on classical imaging operations for this purpose. We developed a tool that supports the annotation of the RPE, see Figure 1, performs the automated classification, and presents a visualization of the result to the user. The architecture of the framework, that relies on software design patterns, allows the fast training, optimization, and adaption to additional patient data sets.

Within an OCT scan, the RPE layer frequently appears as an interrupted and deformable line. We found that a major part of the visible and connected sections of the RPE can be detected by basic image processing operations using single brightness-based thresholds. However, sections with severe damages usually appear at a lower contrast ratio and cannot be distinguished so easily from the surrounding layers of tissue or the choroid. In order to determine connected edge contours that capture high deformations appropriately, we make use of the following conditions:

1. Brightness values of a pixel must reach a specific threshold.

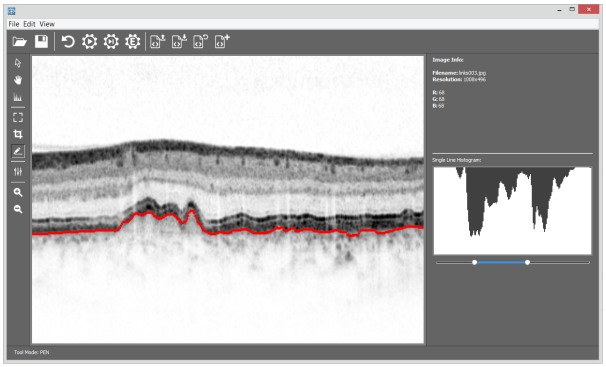

Figure 1: *Graphical user interface of the developed tool allowing for manual annotations, export of annotation meta data as XML, and automated RPE detection (red line). Included is also a parameter optimization for RPE detection as well as batch processing for numerous OCT scans.*

2. Plausibility criterion for continuous edge extraction: While determining the course of the RPE in a pixel-wise manner from left to right, the next candidate on the coordinate should be in the near perimeter of its predecessor with a similar brightness value.
3. Plausibility criterion for retrieval of a segment with a specific length: The neighborhood must contain pixel values that match condition 1.
4. Homogeneous edge extraction: If multiple candidates are found to match conditions 1 to 3, we chose the nearest one with respect to its predecessor.
5. Identification of regions with low contrast: If no candidate is appropriate, we chose the one from the vertical axis that best matches the threshold.

In order to automatically determine the degree of damage in the extracted RPE layer, we investigate the differences between maximum and minimum y-positions of the separate sections and calculate the discrepancy to the ideal slightly curved shape of a healthy person. The combined information about the number and amount of these discrepancies allows us to classify the degree of damage and to eliminate outliers. Here, we use different thresholds that have been trained on given data sets in order to be as accurate and complete as possible. We experience a good performance of this procedure for middle to strong degrees of damage. We propose to visualize the identified RPE damages for all layers as color-coded lines, superimposed to the fundus image. An illustration of the resulting visualization is presented in Figure 2.

4. Data Visualization

In the current clinical work flow, the damage of the macula is typically judged by the distance between the ILM and the RPE layer and summarized in a post-scan report, as illustrated in Figure 3. It can be observed, that these reports violate already simple rules of good visualization practices, e.g. they use ineffective color schemes and even different color schemes within the visualizations of one report, for most of the manufacturers. However, the reports are

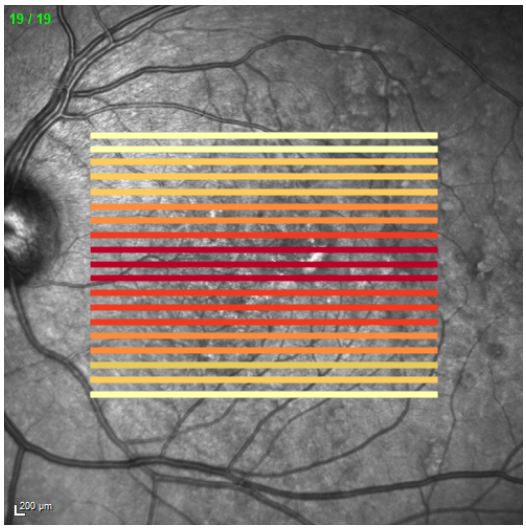

Figure 2: *Visualization of detected RPE damage for one complete 3D OCT scan. The retinal damage is approximated on basis of the curvature of the RPE for each slice. Damage is superimposed to the fundus image at the respective positions of the slices, using a color scheme from bright yellow (no damage) to dark red (massive damage) [HB03].*

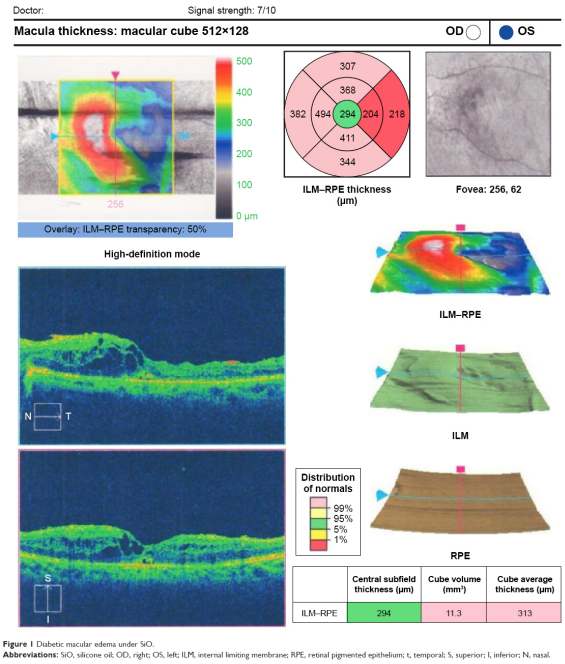

Figure 3: *OCT report, automatically generated by typical OCT scan software for clinical purposes. The report comprises a color-coded ILS-RPE thickness visualization, superimposed to the fundus image (in the upper left part), an ILS-RPE thickness diagram (upper central part), two selected OCT slices with different color coding (lower left part), and a three-dimensional visualization of the extracted retinal layers (middle right part). (Image courtesy of Rashad et al. [RMA16].)*

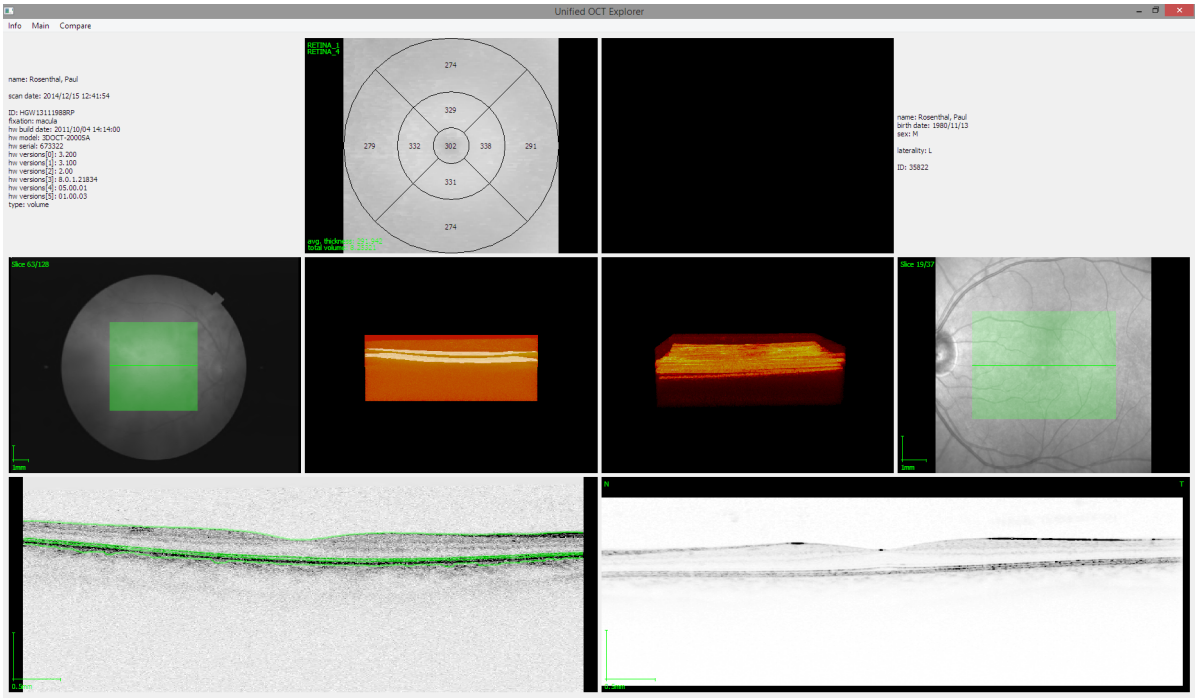

Figure 4: *UOCTE main visualization window with two data sets from the same eye but two different manufacturers loaded. For each data set, the extracted meta data, the ILS-RPE thickness diagram, the fundus image with layer structure, a maximum intensity projection of the 3D data, and a visualization of the current slice are displayed. Two slices can not only be compared in this side-by-side fashion, but also superimposed by a flicker mechanism.*

important for many clinicians and simplify the collected data to a manageable amount. One primarily used visualization for OCT data is the ILS-RPE thickness diagram, shown in the upper central part of Figure 3. Here, the circular area of the macula is divided into the center and two rings with four sectors respectively. An average ILS-RPE thickness is shown as numerical value and encoded as color for each subarea. However, it is unfortunately not documented by most of the manufacturers how the different values are computed exactly. Hence, we again had to investigate different data sets and try several approaches to provide the same functionality in our freely available tool UOCTE.

In addition, we provide some visualization features most of the manufacturers tools are not able to offer. Obviously, UOCTE can be used to compare two different OCT scans from different manufacturers. In this view, we provide a so called blinking, i.e. we display one slice from each of the two data sets alternating, allowing for the effective judgment of changes in the OCT. The visualization interface of UOCTE is illustrated in Figure 4 and furthermore provides an interactive maximum intensity projection view [WMLK89] of the three-dimensional data set. Note that the ILS-RPE diagram is only displayed if both layers are either included in the data or extracted in the preprocessing step.

Apparently, one can apply all possible scalar field visualization techniques to OCT data, once the closed formats are opened. In addition to the maximum intensity projection, we also implemented a marching-cubes based isosurface extraction technique [LC87], see Figure 5. Further widely-used visualization techniques might especially be useful for new research directions in preventive ophthalmology [FSS*15].

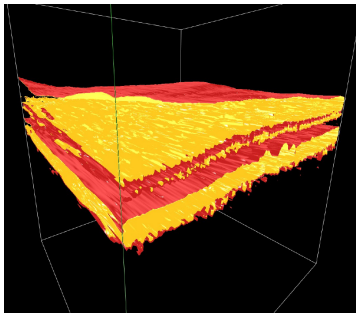

Figure 5: *Two different isosurfaces, colored red and yellow, extracted from OCT data. (Image reproduced from the Master's thesis of Lars Lehmann [Leh15].)*

5. Conclusions

We have presented our findings about the different OCT devices and their generated data with respect to reproducibility. Our tool UOCTE is for the first time able to process multiple different file formats and effectively compare the data of different devices. From the investigations, it is obvious that there are manufacturer-related differences between the OCT scans. In the future, these differences have to be further examined to judge the respective data with respect to its reliability.

Acknowledgments

This work was partially funded by the Novartis Pharma GmbH and the program of Entrepreneurial Regions InnoProfile-Transfer in the project group localizeIT (funding code 03IPT608X).

References

[FSS*15] FUENTES E., SANDALI O., SANHARAWI M. E., BASLI E., HAMICHE T., GOEMAERE I., BORDERIE V., BOUHERAOUA N., LAROCHE L.: Anatomic predictive factors of acute corneal hydrops in keratoconus. *Ophthalmology 122*, 8 (2015), 1653–1659. 4

[HB03] HARROWER M., BREWER C. A.: Colorbrewer.org: An online tool for selecting colour schemes for maps. *The Cartographic Journal 40*, 1 (2003), 27–37. 3

[HSL*91] HUANG D., SWANSON E. A., LIN C. P., SCHUMAN J. S., STINSON W. G., CHANG W., HEE M. R., FLOTTE T., GREGORY K., PULIAFITO C. A., FUJIMOTO J. G.: Optical coherence tomography. *Science 254*, 5035 (1991), 1178–1181. 1

[KRR14] KAHL S., RITTER M., ROSENTHAL P.: Automatisierte Beurteilung der Schädigungssituation bei Patienten mit altersbedingter Makuladegeneration (AMD). In *Proceedings of Forum Bildverarbeitung* (Karlsruhe, 2014), León F. P., Heizmann M., (Eds.), KIT Scientific Publishing, pp. 179–190. 2

[LC87] LORENSEN W. E., CLINE H. E.: Marching cubes: A high resolution 3D surface construction algorithm. In *SIGGRAPH '87: Proceedings of the 14th annual conference on Computer graphics and interactive techniques* (New York, NY, USA, 1987), ACM, pp. 163–169. 4

[Leh15] LEHMANN L.: *Geometrie-basierte Visualisierung von OCT-Daten*. Master's thesis, Technische Universität Chemnitz, 2015. 4

[RMA16] RASHAD M. A., MOHAMED A. A. A., AHMED A. I.: Value of optical coherence tomography in the detection of macular pathology before the removal of silicone oil. *Clinical Ophthalmology 10* (2016), 121–135. 3

[WMLK89] WALLIS J. W., MILLER T. R., LERNER C. A., KLEERUP E. C.: Three-dimensional display in nuclear medicine. *IEEE Transactions on Medical Imaging 8*, 4 (1989), 297–230. 4